

cells to be observed simultaneously. The ability to distinguish each of the luciferases in a mixture, however, is limited by the width of their emissions spectra. From calculations based solely on the overlap of the spectra of the green- and orange-emitting luciferases, one luciferase in a mixture should be detectable in the presence of a 25-fold excess of the other.

library screening and D. R. Helinski for supplying pAD9 and his comments on the manuscript. Supported by NSF grant DMB 8603776 and Office of Naval Research grant N00014-86-K-0267. This

work is dedicated to the memory of Marlene DeLuca, a leader in the field of bioluminescence.

6 December 1988; accepted 7 March 1989

REFERENCES AND NOTES

1. J. W. Hastings, *J. Mol. Evol.* **19**, 309 (1983).
2. H. H. Seliger, J. B. Buck, W. G. Fastie, W. D. McElroy, *J. Gen. Physiol.* **48**, 95 (1964).
3. H. H. Seliger and W. D. McElroy, *Proc. Natl. Acad. Sci. U.S.A.* **52**, 75 (1964).
4. R. A. Crowson, *The Biology of the Coleoptera* (Academic Press, London, 1981).
5. W. H. Biggley, J. E. Lloyd, H. H. Seliger, *J. Gen. Physiol.* **50**, 1681 (1967).
6. *Pyrophorus plagiophthalmus* were collected in Jamaica and frozen in liquid N₂. Polyadenylated RNA was isolated from the abdominal organ; 1 μg was converted to cDNA and inserted into Lambda ZAP to yield 700,000 recombinants, 5.5% of which could express luciferase antigens in *E. coli*. Of 18 phages chosen from the unamplified library by their reactivity with antibody to firefly luciferase, 4 could express bioluminescence in *E. coli*. The library was screened directly for bioluminescent activity from five portions that were amplified and converted into the Bluescript plasmid. Several bioluminescent colonies from each portion were identified by their ability to darken x-ray film; seven were determined as arising from independent cDNA clones. From two of the portions, two sets of colonies were judged as arising from independent clones based on widely different luminescent intensities, which were subsequently confirmed by restriction mapping.
7. J. M. Short, J. M. Fernandez, J. A. Sorge, W. D. Huse, *Nucleic Acids Res.* **16**, 7583 (1988).
8. G. Wienhausen and M. DeLuca, *Photochem. Photobiol.* **42**, 609 (1985).
9. K. V. Wood and M. DeLuca, *Anal. Biochem.* **161**, 51 (1987).
10. The plasmid pKW9 contains the *trp-lac* hybrid promoter (*tac*) and ribosome binding site (RBS) derived from pDR540 (Pharmacia LKB Biotechnology), and a transcriptional terminator derived from pAD9. The replicon portion of the vector is derived from pUC19. The cDNA clones were excised from Bluescript with the Bam HI and Xho I sites of the vector, and inserted into these sites in pKW9 between the *tac* promoter/RBS and the transcriptional terminator. Although the Bam HI site in pKW9 is immediately adjacent to the RBS, the 5' untranslated regions of the cDNAs and a portion of the polylinker region of Bluescript removed the translational initiation codon from the RBS by at least 50 bp. The first ATG encountered downstream of the *tac* promoter is the proper initiation codon for each of the cDNAs, thus reducing spurious initiations and the production of fusion proteins.
11. W. D. McElroy and H. H. Seliger, *Arch. Biochem. Biophys.* **88**, 136 (1960).
12. S. J. Gould, G. A. Keller, S. Subramani, *J. Cell Biol.* **105**, 2923 (1987); *ibid.* **107**, 897 (1988); S. J. Gould *et al.*, *J. Cell Biol.*, in press.
13. M. DeLuca and W. D. McElroy, Eds., *Methods in Enzymology* (Academic Press, Orlando, FL, 1978), vol. 57.
14. J. R. de Wet, K. V. Wood, D. R. Helinski, M. DeLuca, *Proc. Natl. Acad. Sci. U.S.A.* **82**, 7870 (1985); D. W. Ow *et al.*, *Science* **234**, 856 (1986); H. T. Tatsumi, T. Masuda, E. Nakano, *Agric. Biol. Chem.* **52**, 1123 (1988); P. K. Howard, K. G. Ahern, R. A. Firtel, *Nucleic Acids Res.* **16**, 2613 (1988); A. G. DiLella *et al.*, *ibid.*, p. 4159.
15. J. R. de Wet, K. V. Wood, M. DeLuca, D. R. Helinski, S. Subramani, *Mol. Cell. Biol.* **7**, 725 (1987); S. J. Gould and S. Subramani, *Anal. Biochem.* **175**, 5 (1988).
16. We thank S. T. Swanson for assistance with the

Reexamination of the Three-Dimensional Structure of the Small Subunit of RuBisCo from Higher Plants

STEFAN KNIGHT, INGER ANDERSSON, CARL-IVAR BRÄNDÉN

The structure of L₈S₈ RuBisCo (where L is the large subunit and S is the small subunit) from spinach has been determined to a resolution of 2.8 Å by using fourfold averaging of an isomorphous electron density map based on three heavy-atom derivatives. The structure of the S subunit is different from that previously reported for the tobacco S subunit in spite of 75 percent sequence identity. The elements of secondary structure, four antiparallel β strands and two α helices, are the same, but the topology and direction of the polypeptide chain through these elements differ completely. One of these models is clearly wrong. The spinach model has hydrophobic residues in the core between the α helices and β sheet as well as conserved residues in the subunit interactions. The deletion of residues 49 to 62 that is present in the *Anabaena* sequence removes a loop region in the spinach model. The positions of three mercury atoms in the heavy-atom derivatives agree with the assignment of side chains in the spinach structure.

CHAPMAN *et al.* (1) HAVE RECENTLY described the tertiary structure of plant RuBisCo, the key enzyme (2) in the Calvin cycle of carbon dioxide fixation in photosynthesis. Their model is based on an electron density map to 2.6 Å of the L₈S₈ molecule from tobacco. We have determined the structure of L₈S₈ RuBisCo from spinach to 2.8 Å resolution and find very significant differences in the structure of the S subunit compared with the reported tobacco structure. Since there is 75% identity between the amino acid sequences of these two polypeptide chains, they are expected to have similar tertiary structures.

Crystals of spinach RuBisCo that diffract to 1.7 Å resolution were grown from solutions of the activated form of the enzyme with a bound transition-state analogue (3). These crystals contain one-half the L₈S₈ molecule in the asymmetric unit. There is a local noncrystallographic fourfold axis through the molecule, which has approximate 422 symmetry. X-ray data were collected on the synchrotron radiation source in Daresbury, United Kingdom, for the native enzyme and three heavy-atom derivatives. An initial electron density map was calculated with the use of isomorphous phase angles. These were refined by real-space averaging (4) around the local fourfold axis. Data collection procedures and phasing statistics have been briefly described (5).

The final electron density map was of very good quality, as would be expected by fourfold averaging of an electron density map

based on three heavy-atom derivatives. Almost all of the side chains could easily be identified from the known sequences of the spinach S and L chains (6, 7), which comprise 123 and 475 residues, respectively. The sequence of the S subunit, which was determined by amino acid analysis (6), contains only one Cys residue, Cys 112. However, two independent determinations of the amino acid content of the spinach small subunit (8) made in different laboratories have shown that there are three Cys residues per subunit. Furthermore, almost all of the small subunits from higher plant RuBisCo for which the sequences are known contain three Cys residues at positions 41, 77, and 112. We therefore conclude that in all probability the spinach small subunit also contains Cys residues at these three positions. Our electron density map also strongly supports Cys side chains at these positions; the side-chain electron densities are appropriate for Cys (Fig. 1b).

We first built the L chain (5) using the known structure of L₂ RuBisCo from *Rhodospirillum rubrum* (9). We found, in agreement with the work on the tobacco enzyme (1, 10), that higher plant L chains have a structure that is quite similar to that of the bacterial enzyme (9) except at the carboxyl terminal. The arrangement of the L subunits in the spinach enzyme into four L₂ dimers

Swedish University of Agricultural Sciences, Uppsala Biomedical Center, Department of Molecular Biology, S-751 24 Uppsala, Sweden.

around the fourfold axis is also similar to that of the tobacco enzyme. A detailed description of the active site, which is contained within the L subunit, has been published (5).

The electron density corresponding to the S subunit was of equally good quality. There is an unusually high proportion of aromatic residues in the S subunit with nine Tyr, eight Phe, and four Trp residues among the 123 residues of the polypeptide chain. These, together with the three Met residues, provided excellent markers in the electron density map along the continuous density for the polypeptide main chain. Representative examples of the electron density with superimposed skeleton models are given in Fig. 1. We had no difficulties in unambiguously tracing the polypeptide chain and positioning the side chains in appropriate electron density with the BONES option of FRODO (11) on a PS390 computer graphics workstation (coordinates to be submitted to the Brookhaven Data Bank).

The core of the S-subunit structure is a four-stranded antiparallel β sheet of topology (+1, -2 α , -1) with two α helices on one side of the sheet (Fig. 2). The amino-terminal residues form an arm separated from the rest of the subunit structure that extends to a neighboring S subunit and form the only packing contacts between S subunits (Fig. 3). Between β strands 1 and 2, a long loop comprising residues 45 to 66 projects out from the core of the subunit and approaches the molecular fourfold axis. This loop is wedged between two L subunits and forms extensive interactions with these. Following the loop there is a β - α - β motif where the two β strands are separated by one strand within the β sheet. The two α helices pack against the antiparallel β sheet forming a hydrophobic core that comprises residues Leu 26, Val 30, Pro 40, Leu 42, Met 74, Val 83, Val 87, Val 99, Phe 101, Phe 115, and Ala 117. These residues are all invariant or conservatively substituted in all known sequences of the RuBisCo small subunit.

The model of the S subunit described by Chapman *et al.* (1) also contains a core of four antiparallel β strands [figure 2A in (1) and Fig. 4b]. The positions of these β strands in relation to the L subunits agree in the two structures [compare figure 1B in (1) and Fig. 5]. Similarly, the positions of two of the three α helices in the tobacco model agree with our spinach model. However, the topology and direction of the polypeptide chain through these elements of secondary structure differ completely (Fig. 4). The connections agree at one end of the β strands in the topology diagram, but they

are quite different at the other end. Furthermore, the NH₂- and COOH-termini are at quite different positions in the two models. Most of these regions, residues 1 to 6, 38 to 42, and 114 to 123 in the tobacco model (Fig. 4B) have poor density in the tobacco

electron density map according to Chapman *et al.* (1). As a consequence of these different connections, the direction of the polypeptide chain is different through both the β strands and the α helices. All of the amino acid side chains are therefore located in

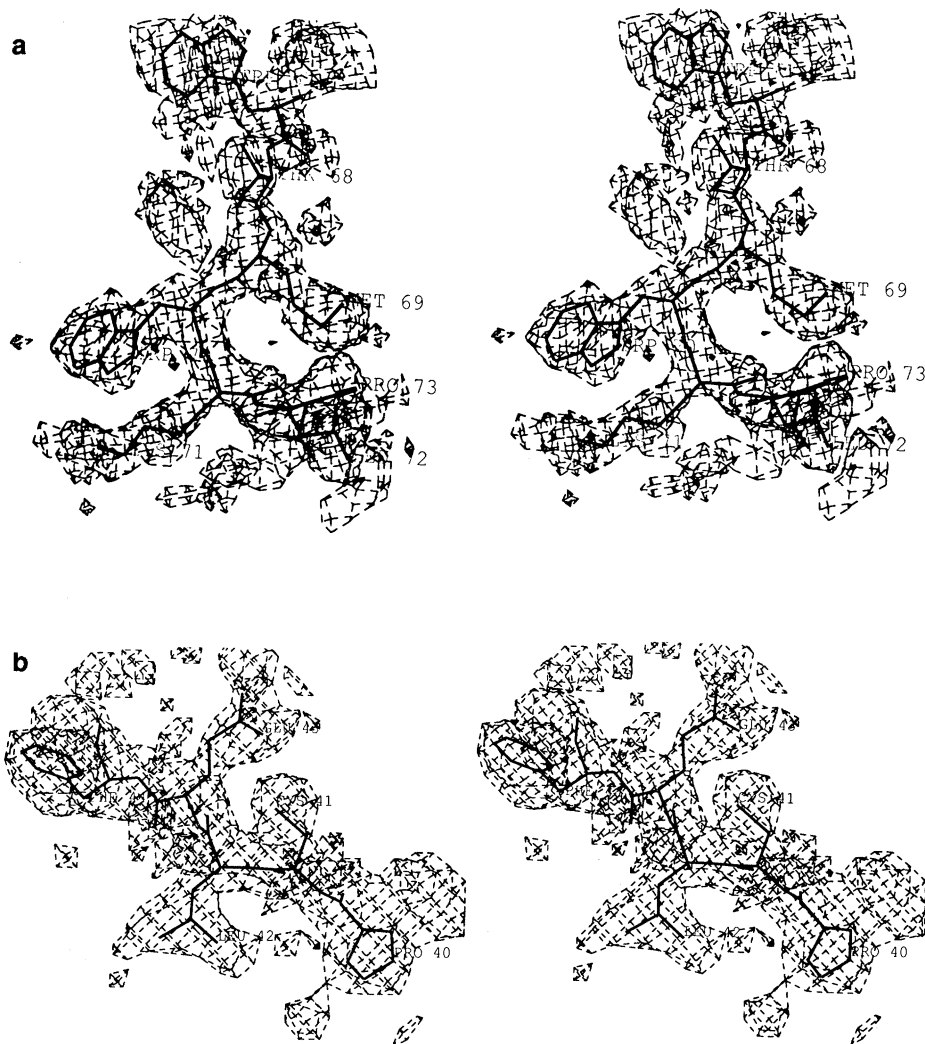


Fig. 1. Examples of electron densities with superimposed skeleton models within the spinach RuBisCo small subunit (14). (a) Residues W 67, T 68, M 69, W 70, K 71, L 72, and P 73. (b) Residues P 40, C 41, L 42, E 43, and F 44 (C 41 is given as Pro in the published sequence; see text).

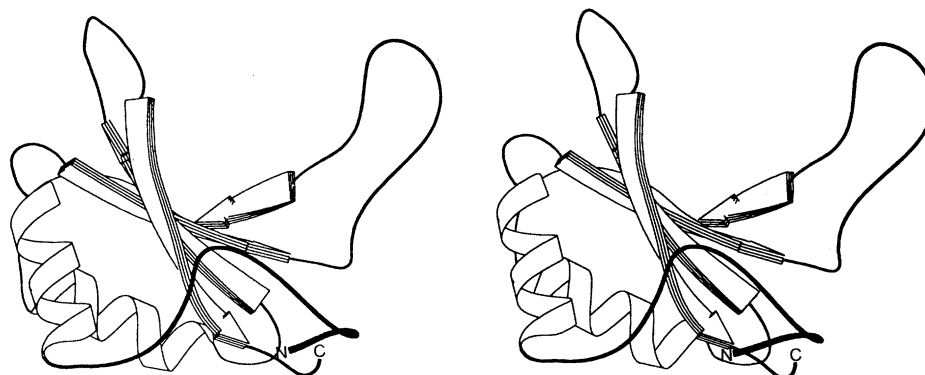


Fig. 2. Stereodigram of a computer-generated (13) schematic ribbon diagram of the S subunit of spinach RuBisCo.

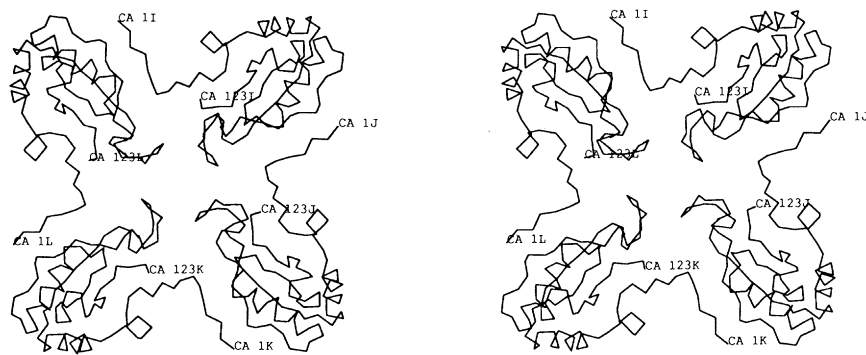


Fig. 3. Stereodiagram of the four S subunits at one end of the spinach L_8S_8 RuBisCo molecule.

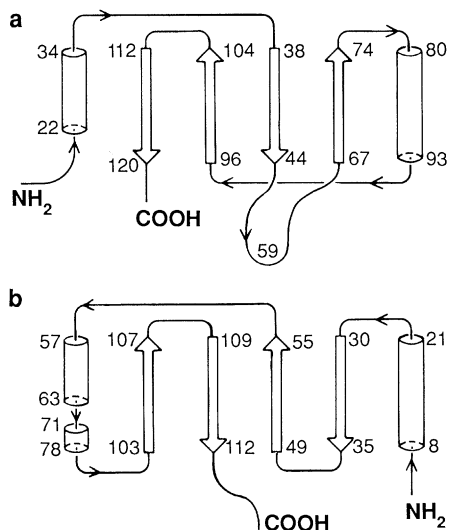


Fig. 4. Comparison of topology diagrams of (a) the spinach model and (b) the tobacco model (1) of the small subunit of RuBisCo. Arrows denote β strands and cylinders α helices. Numbers refer to residue numbers in the amino acid sequence.



Fig. 5. Stereodiagram of one L (thin lines) and one S subunit (thick lines) of L_8S_8 spinach RuBisCo. The view is the same as in figure 2B of (1).

different positions in these two models, although they contain essentially the same elements of secondary structure.

As a further check of our model of the

RuBisCo small subunit structure, we have examined the subunit interactions, the positions of bound Hg atoms from our heavy-atom derivatives in relation to the side

chains, and possible structural effects of the deletion of residues 51 to 62 in RuBisCo from *Anabaena* (Fig. 6). The gross arrangement of the subunits in the L_8S_8 spinach structure is the same as in the tobacco molecule (1, 10). Each S subunit is wedged between two L subunits and forms extensive interactions with these. In addition, it interacts with two neighboring S subunits (Fig. 3) as well as with the N domain of a third L subunit.

Residues of the S subunit that participate in these interactions in our model are mainly from regions of the sequence that are conserved in all higher plants (Fig. 6). There are five regions in the sequence that contain at least three consecutive conserved residues (Fig. 6); 3 to 5, 10 to 19, 49 to 54, 61 to 79, and 101 to 117. Residues in these regions form the majority of the subunit interactions. Residues 3 to 5 interact with residues 68 to 72 of a neighboring S subunit and form the major S-S contacts. Residues 13 to 19, 53, and 57 to 65 form the major interaction area with one of the L subunits, whereas residues 61 to 72 and 101 to 111 interact with the second L subunit. Almost all of the 45 residues from the L chain that participate in these interactions are conserved in all higher plants, and many are also conserved in L_8S_8 RuBisCo from lower photosynthetic organisms. Examples of these strictly conserved interactions are Thr 14S-Arg 167L, Tyr 17S-Arg 421L, Glu 43S-Arg 187L, and Tyr 66S-Phe 220L.

Residues 51 to 62 are deleted in the small subunit of RuBisCo from the cyanobacterium *Anabaena* (Fig. 6). In our model this region corresponds to the extensive loop that projects toward the fourfold axis (Fig. 4). This loop can be deleted without disruption of the core of the subunit structure (Figs. 2 and 4). However, it is involved in the spinach structure in interactions with two L subunits, and a deletion would remove these interactions. Consequently, there would be no constraints in *Anabaena* to conserve residues from the L subunit that are involved in these interactions in RuBisCo from other sources. Two examples of such interactions are hydrogen bonds between the side chains of His 55S and Tyr 226L and from the side chain of Arg 53S to the main chain O of Gly 261L. In all higher plants these residues are conserved, but they have mutated to Thr226L and Lys 261L in *Anabaena*. If these mutated residues would occur in RuBisCo molecules with a conserved loop region, the hydrogen bonds could not be formed and, in addition, the subunit packing arrangement would be severely distorted.

Heavy-atom positions that are used to obtain isomorphous phase angles are located

```

1      11
a M Q V W P P L G L K K F E T L S Y L P P
b . . V W P . . . . K K . E T L S Y . P .
c M Q T L P . . . K E R R Y E T L S Y L P P

21     31
a L T T E Q L L A E V N Y L L V K G W I P
b . . . . L . . . W . P . Y L . . Y . W . P .
c L T D V Q I E K Q V Q Y I L S O G Y I P

41     51
a P L E F E V K D G F V Y R E H D K S P G
b C . E F . . . G F V . R E . . . S P .
c A V E P N E V S E F . . . . .

61     71
a Y Y D G R Y W T M W K L P M F G G T D P
b Y Y D G R Y W T M W K L P M F G G T D P
c . . T E L Y W T L W K L P L F G A K T S

81     91
a A Q V V N E V E E V K K A P P D A F V R
b . . Q V . . E . . E . . . Y P . . . R R
c R E V L A E V Q S C R S O Y P G H Y I R

101    111
a F I G F N D K R E V Q C I S F I A Y K P
b . I G F D N . R Q V Q C . . F I A . . P P
c V V G F D N I K Q C Q I L S F I V H K P

121
a A G Y
b . . .
c S R Y

```

Fig. 6. Amino acid sequences of the small subunit of RuBisCo molecules. (a) Sequence of spinach S subunit (6). (b) Invariant residues in S subunits from other higher plants. [Data taken from the NBRF Protein Data Bank.] Residues that vary are indicated by dots. (c) Amino acid sequence of the S subunit from *Anabaena* RuBisCo (12). Residues 6, 7, and 51 to 62 are deleted.

without any prior knowledge of the protein structure, and therefore they provide independent evidence for a correct chain tracing if chemically proper side chains are found in the binding sites. Mercury compounds usually bind to accessible Cys residues. The Hg complexes that we used in spinach RuBisCo, ethyl mercury thiosalicylate and $K_2Hg(CN)_4$, bind to seven different sites, four in the L chain and three in the S chain. All four Hg binding sites in the L chain contain Cys residues; Hg1 binds to Cys 84L and His 86L, Hg2 to Cys 172L as well as Cys 192L, Hg3 to Cys 427L and Met 387L, and Hg4 to Cys 459L. In the S chain we find that one Hg binds to Cys 112 as well as to the N atom of Trp 38. The other two Hg binding sites are adjacent to residues 41 and 77. Granted that these are Cys residues, the three different Hg atoms in the S subunit bind to the three Cys residues providing independent support for our chain tracing. Corresponding residues in the tobacco chain tracing are in quite different regions of the molecule (Fig. 4) and do not agree with our observed Hg positions.

REFERENCES AND NOTES

1. M. S. Chapman *et al.*, *Science* **241**, 71 (1988).
2. H. M. Mizioro and G. H. Lorimer, *Annu. Rev. Biochem.* **52**, 507 (1983).
3. The crystals belong to space group C222₁, with cell dimensions $a = 157.2$ Å, $b = 157.2$ Å, and $c = 201.3$ Å [I. Andersson and C.-I. Brändén, *J. Mol. Biol.* **172**, 363 (1984)].
4. G. Bricogne, *Acta Crystallogr.* **A32**, 832 (1976).
5. The R_{sym} value of the 70,765 independent reflections to 2.4 Å resolution from 175,242 measurements of the native data was 4.9%. Phase angles were calculated for 52,318 reflections, which com-

prise 83% of the total number of reflections between 10 and 2.8 Å resolution. The figure of merit was 0.51 for the multiple isomorphous replacement (MIR) phases. After the fourfold molecular averaging, the final R-value was 0.16 and the root-mean-square (rms) phase change was 63° [I. Andersson *et al.*, *Nature* **337**, 229 (1989)].

6. P. G. Martin, *Aust. J. Plant Physiol.* **6**, 401 (1979); I. Takuri *et al.*, *Phytochemistry* **20**, 413 (1981).
7. G. Zurawski, B. Perrot, W. Bottomley, P. R. Whitfeld, *Nucleic Acids Res.* **9**, 3251 (1981).
8. T. Takabe and T. Akazawa, *Arch. Biochem. Biophys.* **169**, 686 (1975); G. Lorimer, unpublished results.
9. G. Schneider, Y. Lindqvist, C.-I. Brändén, G. Lorimer, *EMBO J.* **5**, 3409 (1986).

10. M. S. Chapman *et al.*, *Nature* **329**, 354 (1987).
11. T. A. Jones and S. Thirup, *EMBO J.* **5**, 819 (1986).
12. S. A. Nierzwicki-Bauer, S. E. Curtis, R. Haselkorn, *Proc. Natl. Acad. Sci. U.S.A.* **81**, 5961 (1984).
13. J. P. Priestle, *J. Appl. Cryst.* **21**, 572 (1988).
14. Abbreviations for the amino acid residues are: A, Ala; C, Cys; D, Asp; E, Glu; F, Phe; G, Gly; H, His; I, Ile; K, Lys; L, Leu; M, Met; N, Asn; P, Pro; Q, Gln; R, Arg; S, Ser; T, Thr; V, Val; W, Trp; and Y, Tyr.
15. Supported by grants from the Swedish Research Councils NFR and SJFR as well as from E. I. du Pont de Nemours and Co. USA.

3 January 1989; accepted 28 February 1989

Receptor-Mediated Drug Delivery to Macrophages in Chemotherapy of Leishmaniasis

AMITABHA MUKHOPADHYAY, GAUTAM CHAUDHURI,*
SUNIL K. ARORA, SHOBHA SEHGAL, SANDIP K. BASU†

Methotrexate coupled to maleylated bovine serum albumin was taken up efficiently through the "scavenger" receptors present on macrophages and led to selective killing of intracellular *Leishmania mexicana amazonensis* amastigotes in cultured hamster peritoneal macrophages. The drug conjugate was nearly 100 times as effective as free methotrexate in eliminating the intracellular parasites. Furthermore, in a model of experimental cutaneous leishmaniasis in hamsters, the drug conjugate brought about more than 90% reduction in the size of footpad lesions within 11 days. In contrast, the free drug at a similar concentration did not significantly affect lesion size. These studies demonstrate the potential of receptor-mediated drug delivery in the therapy of macrophage-associated diseases.

LEISHMANIASIS, A PARASITIC disease, is estimated to affect 400,000 to 12 million people worldwide annually (1, 2). The causative agents of leishmaniasis, the various *Leishmania* species, reside and proliferate solely in mammalian host macrophages (3). Currently used drugs for chemotherapy of leishmaniasis, such as antimonials, amphotericin B, and pentamidine, can produce severe toxic side effects and relatively high relapse rates occur (4, 5). Such side effects are presumably due to the interaction of the drugs with different cell types of the host, including those not harboring the parasites. Antimonials, amphotericin B, and pentamidine encapsulated in liposomes were more effective than free drugs for the treatment of leishmaniasis in experimental model systems (6–10). Even in

these earlier studies, liposomes that did not carry drugs showed appreciable toxic effects (11). In this report we describe an alternative modality for selective delivery of drugs to macrophages in which a cytotoxic drug, methotrexate (Mtx), was coupled to a macromolecular ligand, maleylated bovine serum albumin (MBSA), recognized by the "scavenger" receptors reported to be present primarily on the cells of macrophage lineage (12–14). The superior leishmanicidal activity of this drug conjugate in eliminating intracellular amastigotes of *Leishmania mexicana amazonensis* both in vitro and in vivo demonstrates the efficacy of this approach.

For preparation of the drug conjugate, water-soluble carbodiimide was used to couple MBSA chemically with unlabeled or tritiated Mtx (15, 16). Mtx-MBSA containing 35 moles of Mtx per mole of MBSA was used in these studies. The kinetics of uptake of free and conjugated Mtx by cultured macrophages derived from peritoneal fluid of hamsters are shown in Fig. 1. At an Mtx concentration of 3 µg/ml in the medium, either in free or conjugated form, the intracellular content of Mtx was 70 ng and 279 ng per milligram of cellular protein, respectively, after 3 hours of incubation. The uptake of Mtx-MBSA exhibited saturation

A. Mukhopadhyay, G. Chaudhuri, S. K. Basu, Institute of Microbial Technology, 1389, Sector 33 C, Chandigarh-160 031, India.
S. K. Arora and S. Sehgal, Post Graduate Institute of Medical Education and Research, Chandigarh-160 012, India.

*Present address: Department of Microbiology and Immunology, University of Health Sciences, Chicago Medical School, 3333 Green Bay Road, North Chicago, IL 60064.

†To whom correspondence should be addressed.